"INCOHERENT DETECTION"

Royal Norwegian Council for Scientific and Industrial Research

45

EVENT DETECTION PROBLEMS USING A PARTIALLY COHERENT SEISMIC ARRAY

by

F. Ringdal, E.S. Husebye
and A. Dahle

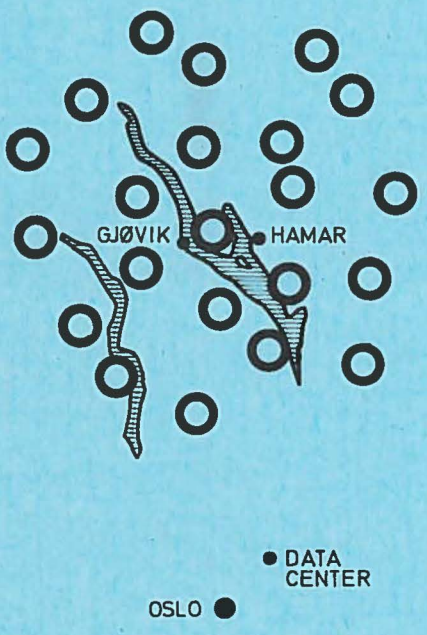

NORWEGIAN SEISMIC ARRAY

NORSAR

P. O. Box 51. 2007 Kjeller – Norway

NTNF/NORSAR
Post Box 51
N-2007 Kjeller
NORWAY

NORSAR Technical Report 45

45

EVENT DETECTION PROBLEMS USING A PARTIALLY COHERENT SEISMIC ARRAY

by

F. Ringdal, E.S. Husebye
and A. Dahle

20 December 1972

The NORSAR research project has been sponsored by the United States of America under the overall direction of the Advanced Research Projects Agency and the technical management of Electronic Systems Division, Air Force Systems Command, through contract no. F19628-70-C-0283 with the Royal Norwegian Council for Scientific and Industrial Research.

This report has been reviewed and is approved.

Richard A Jedlicka, Capt USAF
Technical Project Officer
Oslo Field Office
ESD Detachment 9 (Europe)

ABSTRACT

Seismic event detection by conventional beamforming does not always produce good results for a large aperture seismic array. This may be due to poor signal coherency or beamforming loss by missteering. An "incoherent beamforming detector" is described in this paper as a method to improve array detectability in such cases. This detector, which essentially consists of beamforming on P-wave envelopes, has been implemented in the NORSAR processing system and relevant results are presented and discussed in this paper. The incoherent detector is shown to be superior to the conventional in detecting near regional events and underground explosions. The statistical distribution of signal amplitudes across a network of sensors is found to be lognormal. Implications of this factor on event detectability by conventional and incoherent beamforming are discussed.

1. INTRODUCTION

The continuous operation of a large aperture seismic array requires a device for automatically detecting incoming signals generated by earthquakes and underground explosions. The obvious reason for this is the large number of beams that must be deployed to ensure adequate surveillance of the global seismic activity. The individual array beams, which are essentially phased sums of single sensor traces, have to be monitored continuously to identify possible arrivals of seismic wave energy.

The main problem encountered when designing an automatic event detector is to maximize signal-to-noise ratio (SNR) for seismic signals relative to the variability of the seismic noise. Several factors have to be considered to achieve this goal. Bandpass filtering makes it possible for the detector to operate in that part of the frequency domain where SNR is best in average. For individual sensor traces at NORSAR, this is known to occur at fairly high frequencies, i.e., around 2 Hz. The variability of the seismic noise,

and thereby the false alarm probability, has been shown by Lacoss (1972) to be lowest for high filter frequency. On the other hand, array beamforming loss increases sharply with increasing signal frequency, thus necessitating a trade-off between the above factors to improve array detectability. Another factor complicating the array response is the large signal amplitude variations between sensors which in extreme cases may reach a factor of 20. Typically, a few sensors may be consistently good for events in one seismic area, but consistently poor for other regions.

The purpose of this paper is to discuss some topics relevant to seismic array event detection. In particular we want to present results from the "incoherent beamforming detector" implemented at the NORSAR data center by NTNF personnel in 1972. This detector, which was first suggested

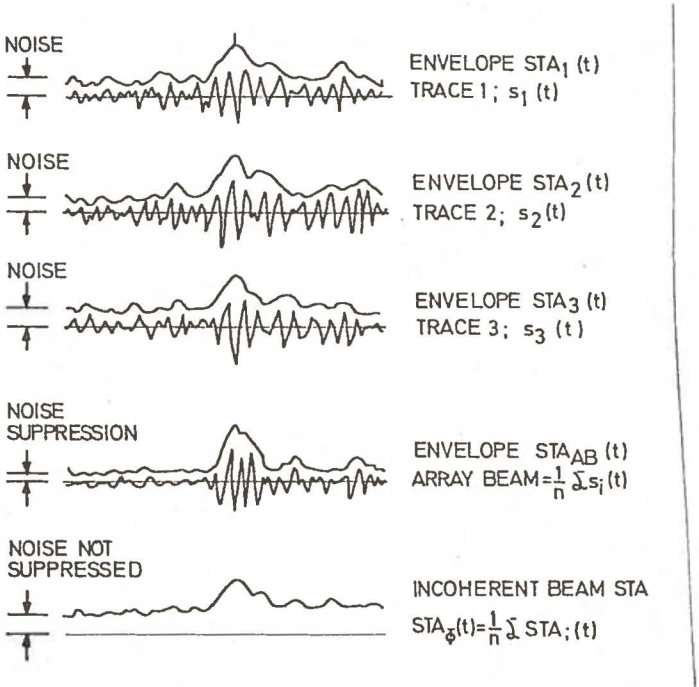

Fig 1. Principles of coherent and incoherent beamforming. The signal envelopes represent STA values over a 1.5 second sliding integration window.

by Felix et al (1972), consists in principle of forming the so-called incoherent array beams by adding together envelopes of subarray beams after proper time delays have

been introduced (see Fig 1). We also investigate theoretically the statistical amplitude distribution across a seismic array, and present some implications of this factor for the event detectability.

In Section 2 event detectors will be discussed in general, while Section 3 deals more closely with the relationship between coherent and incoherent beams. A seismic event detectability comparison is worked out in Section 4. In Section 5 a theoretical explanation of the observed log-normal signal amplitude distribution across a network of sensors is given. Finally, relevant data analysis is presented in Section 6 to test the theoretical models described previously on real seismic signal data. Section 7 gives a brief discussion of the obtained results.

2. EVENT DETECTOR DESIGN

The fundamental characteristics of an array is its capability of suppressing ambient noise by beamforming. In practice, a sensor spacing of minimum 3-4 km and an array diameter of up to a few hundred kilometers ensures uncorrelated noise between sensors while retaining reasonable signal coherency across the array. The NORSAR array has been constructed according to this principle. For a more detailed description of the NORSAR hardware and software, we refer to Bungum et al (1971).

The event detector implemented by IBM personnel is a conventional beamforming detector, deploying around 300 array beams in real time. Prior to the beamforming, all sensors have been bandpass filtered for additional noise suppression. A near-continuous signal-to-noise ratio test is applied to each individual beam, the signal and noise estimates being based on rectified and averaged amplitudes. In the following, these estimates have been denoted short term average

(STA) and long term average (LTA) respectively. Theoretically, a detector using signal power estimates should be superior to the linear detector, but the practical difference between the two methods appears to be insignificant (Berteussen, 1972).

Mathematically, the array beamforming may be formulated as follows:

$$AB_C(t) = \sum_{i=1}^{N} S_i(t-\tau_i) \qquad (1)$$

where $S_i(t)$ is the filtered seismometer trace and τ_i is the appropriate beamforming time delay, i = 1,2,...N.

The short term beam average STA_C is then computed as follows

$$STA_C(t) = \sum_{i=1}^{IW} |AB_C(t-i+1)| \qquad (2)$$

STA_C at time t is computed from the last IW AB_C-samples

where IW is integration window in deciseconds, typically 15.

The principle of the incoherent detector is to invert the sequence of beamforming and rectification. Mathematically:

$$AB_I(t) = \sum_{i=1}^{N} |S_i(t-\tau_i)| \qquad (3)$$

NB absolute values!

$$STA_I(t) = \sum_{i=1}^{IW} AB_I(t-i+1) \qquad (4)$$

In the NORSAR on-line system, array beamforming has been implemented as a two-step process, the first step being subarray beamforming for each of the 22 subarrays. Signal

coherency across a subarray is in general much better than between subarrays. As is shown in Section 3, the incoherent beamforming method is superior to conventional beamforming only if signal coherency is poor. Consequently, it was decided to implement an incoherent detector based on rectified subarray beams rather than single sensor traces in the NORSAR Detection Processor.

The incoherent beamforming method is able to take advantage of high SNR in high frequency bands observed at NORSAR. In the initial implementation, a 1.6-3.2 Hz bandpass filter was used in connection with this method, while the conventional beamforming filter was 1.2-3.2 Hz at the time.

Several other detectors have been developed for seismic arrays, but lie outside the scope of this article. We restrict ourselves to briefly mentioning the Fisher detector which was first suggested by Melton and Bailey (1957). The operating principle of this detector is to subtract each signal trace from the beam, and then divide the beam power with the average power of all such differences. This detector has a well-known statistical distribution, and has been demonstrated in an operational mode (Edwards et al 1967). The Fisher detector requires coherent signals across the array and well-equalized amplitude responses between sensors for optimum performance.

3. COHERENT AND INCOHERENT BEAMFORMING

In this section we will study the relationship between signal-to-noise ratios for the coherent and incoherent beams. Suppose n channels are available for the beamforming process. The time series may e.g. be filtered seismometer traces, filtered subarray beams or a combination. During noise conditions the channels are assumed to be independent, stationary Gaussian processes $N_i(t)$,

$i=1,\ldots,n$. The occurrence of a seismic signal implies an additional term $S_i(t)$ to be added to each channel. We assume also that the $S_i(t)$ are Gaussian processes of short duration.

The signal-to-noise ratios SNR_C and SNR_I for coherent and incoherent beams respectively are defined as the quotients between a short term average (STA) and long term average (LTA) for the beams. The STA and LTA are calculated by averaging the rectified beams over short (typically 1.5 seconds) and long (typically 30 seconds) periods of time. A detection is declared if SNR_C or SNR_I exceed predefined thresholds. Note that SNR_I and SNR_C are well defined whether or not a seismic signal is present. We will now develop the relationship between SNR_I and SNR_C when a seismic signal occurs and assume that

$$STA(S_i+N_i) = c\cdot\sigma(S_i+N_i) \qquad i=1,\ldots,n \quad (5)$$

$$LTA(N_i) = c\cdot\sigma(N_i) \qquad i=1,\ldots,n$$

where σ denotes the standard deviation of the Gaussian process and c is a constant. For simplicity, the time variable is $S_i(t)$ and $N_i(t)$ has been omitted. Note that (5) is a reasonable assumption since $E(|X|)$ is proportional to σ when X is Gaussian (o,σ).

average of a rectified variable

In the coherent case this yields:

$$SNR_C = \frac{STA\left(\sum_{i=1}^{n}(S_i+N_i)\right)}{LTA\left(\sum_{i=1}^{n}N_i\right)} = \frac{\sigma\left(\sum_{i=1}^{n}(S_i+N_i)\right)}{\sigma\left(\sum_{i=1}^{n}N_i\right)} =$$

$$= \left[1+\frac{\sigma^2\left(\sum_{i=1}^{n}S_i\right)}{\sigma^2\left(\sum_{i=1}^{n}N_i\right)}\right]^{\frac{1}{2}} \qquad (6)$$

Since noise is independent between channels: (completely incoherent)

$$\sigma^2\left(\sum_{i=1}^{n}N_i\right) = \sum_{i=1}^{n}\sigma^2(N_i)$$

For the signal we will introduce a parameter q by setting

$$\sigma\left(\sum_{i=1}^{n}S_i\right) = \sqrt{q}\cdot\sum_{i=1}^{n}\sigma(S_i) \qquad (7)$$

$$\Downarrow$$

$$\sigma^2\left(\sum_{i=1}^{m}S_i\right) = q\left\{\sum_{i=1}^{m}\sigma(S_i)\right\}^2$$

The variable q lies between 0 and 1, and depends upon signal coherency as well as sampling loss and channel misalignment. If sampling and alignment losses can be disregarded, q is related to the average signal cross-correlation $\bar{\rho}$ through the standard gain formula for seismic arrays:

$$q = \frac{1}{N} + \left(1-\frac{1}{N}\right)\bar{\rho} \qquad (8)$$

By combining eq. (5), (6) and (7) the result is

$$SNR_C = \left[1+q \cdot \frac{\left\{ \sum_{i=1}^{n} \sqrt{STA_i^2 - LTA_i^2} \right\}^2}{\sum_{i=1}^{n} LTA_i^2} \right]^{\frac{1}{2}} \qquad (9)$$

where $LTA_i = LTA(N_i)$ and $STA_i = STA(S_i + N_i)$.

In the simplified case that all $LTA_i = LTA$ and all $STA_i = STA$, $i=1,\ldots,n$, eq. (9) reduces to:

$$SNR_C = [1+n \cdot q((\frac{STA}{LTA})^2 - 1)]^{\frac{1}{2}} \qquad (10)$$

For incoherent beamforming, the loss due to signal incoherency and misalignment is assumed to be negligible, and we may then write:

$$SNR_I = \sum_{i=1}^{n} STA_i / \sum_{i=1}^{n} LTA_i \quad \text{or} \quad SNR_I = STA/LTA \qquad (11)$$

in the simplified case considered above.

A combination of eq. (10) and eq. (11) gives:

$$SNR_C = [1+n \cdot q(SNR_I^2 - 1)]^{\frac{1}{2}} \qquad (12)$$

Thus we have developed a relationship between coherent and incoherent signal-to-noise ratio, assuming that identical bandpass filters are being used and that all sensors are well equalized.

4. DETECTABILITY CONSIDERATIONS

A theoretical comparison between Receiver Operating Characteristics (ROC) for the two beamforming methods requires a knowledge of the statistical distributions of STA_C and STA_I during noise conditions. Experimentally, it seems reasonable to assume that STA of either a single channel or a coherent beam is lognormally distributed, i.e., log{STA} is a Gaussian random variable (Lacoss, 1972). STA_C may therefore be considered lognormal. However, in the incoherent case, we have to consider a sum of independent (lognormal) variables, and by the Central Limit Theorem, STA_I will approach a Gaussian distribution as the number of channels (n) becomes large.

As a first order approximation to a ROC evaluation, we will consider the "normalized" variables:

$$X_I = (STA_I - E(STA_I))/\sigma(STA_I) \quad \text{and}$$

$$X_C = (STA_C - E(STA_C))/\sigma(STA_C) \tag{13}$$

σ and E denote the statistical standard deviation and expectation of the time series STA_I and STA_C during stationary noise conditions.

For a given seismic event, the values of X_I and X_C will then tell how "well" the event can be detected by the two methods.

It is not difficult to see that:

$$\frac{\sigma(STA_C)}{E(STA_C)} = \sqrt{n} \cdot \frac{\sigma(STA_I)}{E(STA_I)} \tag{14}$$

In other words, the incoherent beam suppresses "noise variability" by a factor $\sqrt{n}$, while the coherent beam of course suppresses "noise level" by $\sqrt{n}$.

NB !

Setting $STA_I/E(STA_I) = SNR_I$ and $STA_C/E(STA_C) = SNR_C$ and combining expressions (13) and (14) with expressions (10) and (11) we obtain:

$$R = \frac{X_C}{X_I} = q \cdot \sqrt{n} \cdot \frac{1+\sqrt{1+(SNR_C^2-1)/nq}}{1 + SNR_C} \qquad (15)$$

The ratio R is sketched in Fig 2 for n=22 and different values of q. From this figure it can be seen that unless q is very small, the conventional beamforming has a better detectability for small events. Even with q=0.5 the coherent detector is better for events close to the NORSAR

: R > 1

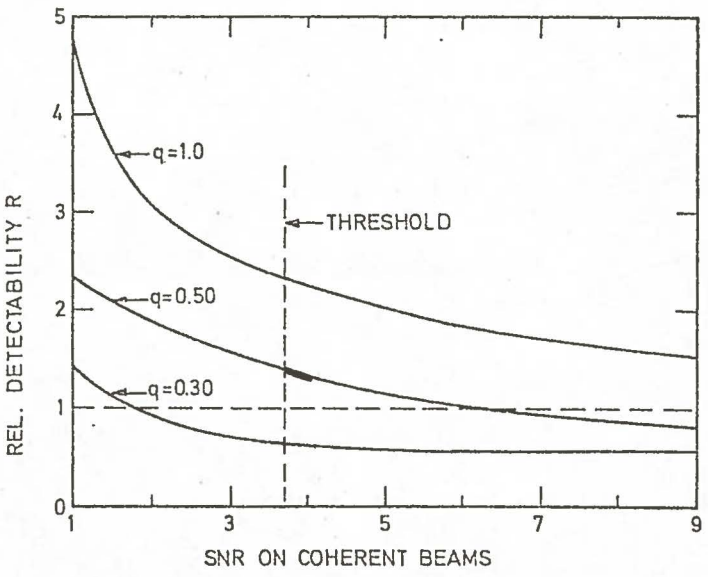

q depends on:
signal coherency
signal loss
channel misalignment
$0 \leq q \leq 1$

Fig 2. Seismic event detectability comparison between coherent and incoherent array beams as defined in eq. (15). Only for small q-values will incoherent beamforming be superior to coherent beamforming.

false alarm threshold (SNR_C 3.5 to 4.0). Thus only in cases of poor signal coherency, the incoherent detector can be expected to contribute to an array's theoretical detection

: low q

capability. In practical operation, however, the narrow main lobes of the coherent array beams makes the conventional beamforming vulnerable to loss due to missteering. It should be noted that the main advantage of incoherent beamforming is its good areal coverage due to the relatively long periodic nature of the envelope traces (see Fig 1). Thus in an operational environment, where only a limited number of beams may be deployed, the picture will turn out to be greatly more favorable to incoherent beamforming than indicated from the theoretical model.

5. AMPLITUDE DISTRIBUTION

Seismic recordings by laterally distributed seismometers from an arbitrary event show a substantial scatter in P-wave amplitudes. It is reasonable to assume that the size of a specific signal amplitude is tied to the ray path from focus to the sensor site. In this respect we may consider the geological structures that a ray "sees" as a layered earth model consisting of N discontinuities. When traversing the i-th interface, the signals will be modified by a transmission coefficient R_i of which a first order approximation may be expressed as:

$$R_i = 1 - \frac{K_i - L_i}{K_i + L_i} \tag{16}$$

where K_i and L_i are functions of the angle of incidence, velocity and density contrasts at the i-th discontinuity. The corresponding amplitude modulation effect is:

$$A_i = R_i A_{i-1} \tag{17}$$

The above argument leads to the expression

$$A = R_N \cdot R_{N-1} \cdots R_1 A_0 \tag{18}$$

where $A=A_N$ is the observed amplitude. Thus, the reconstruction of an observed P-wave amplitude might be regarded as the joint, multiplicative effect of N mutually independent causes, acting in an ordered sequence and depending on the geological structures encountered along the ray path. If signals from a seismic event are received at several stations, a set of such transmission coefficients R_i will apply to each receiving site. For each discontinuity surface, the corresponding transmission coefficient for each station is considered as a random value drawn from some common probability distribution characterized by the ray paths and the geological conditions at the boundary. Sufficient station separation will ensure that these values are statistically independent.

Taking the logarithm on both sides of (18) gives:

$$\log A = \log R_N + \log R_{N-1} + \ldots \log R_1 + \log A_0 \qquad (19)$$

$$= \sum_{i=1}^{N} \log R_i + \log A_0$$

The right hand side of (19) is now a sum of independent variables, and considering N a large number, we infer by the Central Limit Theorem that log A is normally distributed. If log A is normally distributed (m,σ), it is easily seen that the variable A itself has the probability density function

$$\frac{1}{A} \cdot \frac{1}{\sigma\sqrt{2\pi}} e^{-\frac{(\log A - m)^2}{2\sigma^2}} \qquad A > 0 \qquad (20)$$

$$0 \qquad A \leq 0$$

Purposely, the above discussion is tied to short periodic P-waves in the teleseismic range as such signals are likely to "see" many more discontinuities than long periodic P and S waves. Moreover, attenuation and geometrical spreading effects were ignored in view of the wave type considered. In short, observed P-wave amplitudes across a global seismic network or a large array like LASA or NORSAR are expected to be lognormal. In Fig 3 the actual amplitude distribution across the NORSAR array for a typical seismic event is shown, together with normal and lognormal frequency functions fitted to the observed data.

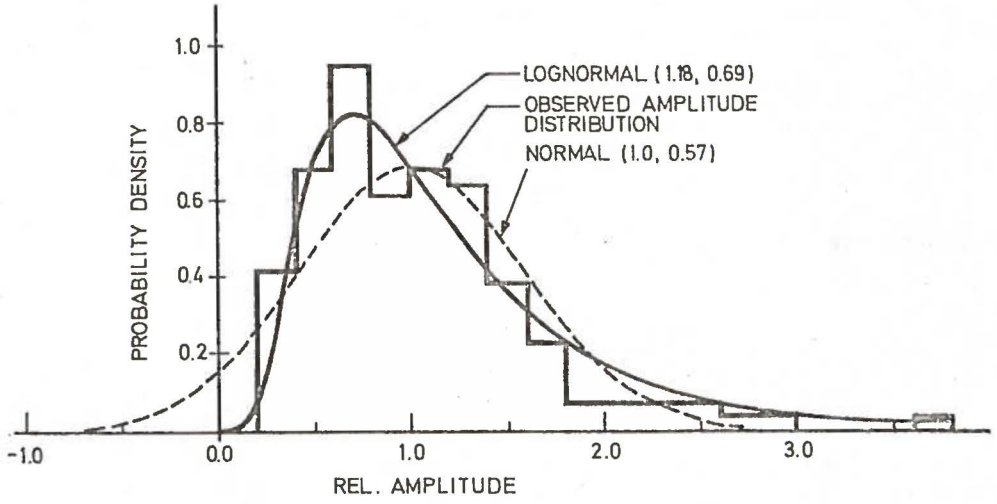

Fig 3. Observed positive amplitude distribution for an Aleutian Island earthquake with a 1.4-3.8 Hz filter (Event No. 2 in Table 4). The normal and lognormal distribution functions estimated from the observed sample mean and variance are also shown.

6. DATA ANALYSIS

The on-line implementation of the incoherent beamformer at NORSAR early in 1972 made it possible to monitor closely the performance of this detector over an extended period of time. To verify the relationship between signal-to-

noise ratios for coherent and incoherent beams developed in Section 3, 81 small and medium size events from Kamchatka region were selected. A 1.2-3.2 Hz bandpass filter was used for prefiltering of both types of beam traces. The signal-to-noise ratios for these events as determined by the Detection Processor are shown in Fig 4. It appears that the observed data fit the theoretical model reasonably well. The low q-values implied from the above figure are mainly caused by the distance separation between the prefixed beam locations and more randomly distributed event locations.

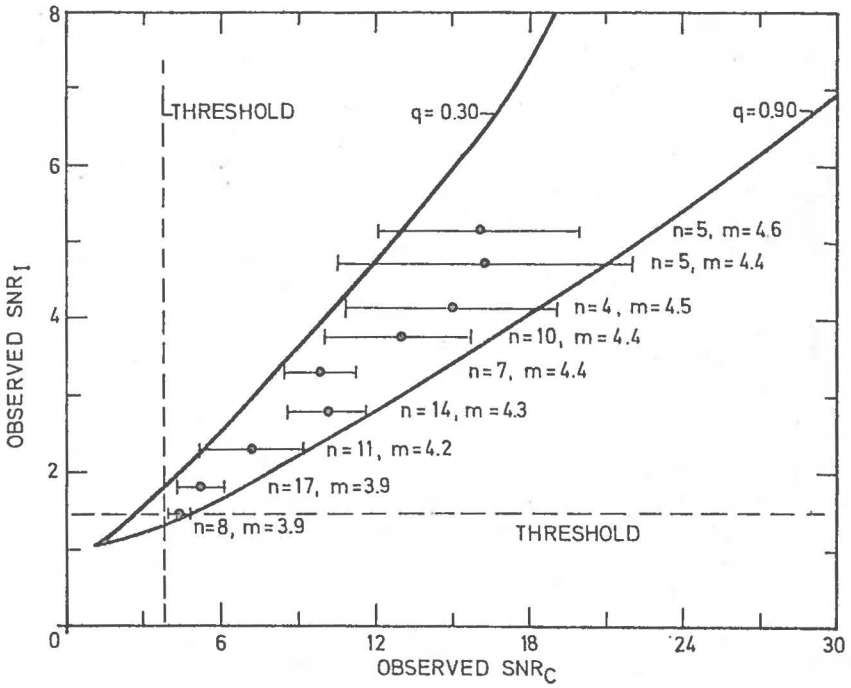

Fig 4. A comparison of SNR values on the coherent and incoherent array beams as reported by the NORSAR on-line event detector. The 81 earthquakes analyzed occurred in the Japan, Kurile Is., Kamchatka and Aleutian Is. regions in the interval Jan-Mar 1972. Altogether 30 coherent and 3 incoherent array beams were deployed in the above regions, using a 1.2-3.2 Hz bandpass filter. In the figure n is the number of events within a certain SNR_I interval while m is the corresponding average of $NORSAR^I$ observed P-wave magnitudes for the n events.

A full-scale incoherent beamforming processor, with a 1.6-3.2 Hz filter, was implemented in the NORSAR Detection and Event Processing system from 16 Sept 1972. This was done while retaining the conventional beamforming detector, which is operated with a 1.2-3.2 Hz filter. Results from the first two months of parallel operation are presented in Fig 5-7, and relevant comments are as follows:

Incoherent beamforming event detection is definitely superior to that of conventional beamforming in the Mediterranean area. This is the case in Western Russia as well, where the conventional beam coverage is poor and the events detected are probably explosions. Also in the Pakistan-Afghanistan region incoherent beams show a better performance. Elsewhere, conventional beamforming, generally, seems to be superior. As to the total number of events detected by the two detectors, regionalization is again instructive as demonstrated in Table 1. Coherent beamforming shows the best performance as expected (see Section 4), but this advantage disappears when only high quality events are considered. Here "high quality events" refers to clean signal arrivals and does not necessarily imply high SNR values.

ZONE No.	Name	EVENTS Total No.	COH.BF Only No.	INC.BF Only No.	COH.&INC. No.	COH. BF Total No.	%	INC. BF Total No.	%
1	Greece/Turkey	117	5	45	67	72	62	112	96
2	USSR/Cent. Asia	194	28	41	125	153	79	166	86
3	Japan/Kam./Aleu.	168	40	7	121	161	96	128	76
4	USA/Cent. America	64	31	1	32	63	99	33	51
5	Global I (All Events)	1038	242	133	663	905	87	796	77
6	Global II (High Quality Events)	546	24	25	497	521	95	522	95

Table 1

Events reported in the NORSAR seismic bulletin, 16 Sep - 15 Nov 1972. The table gives the total number and percent of events detected in different regions by the coherent and incoherent beamforming as well as the number of events detected only by one of these detectors.

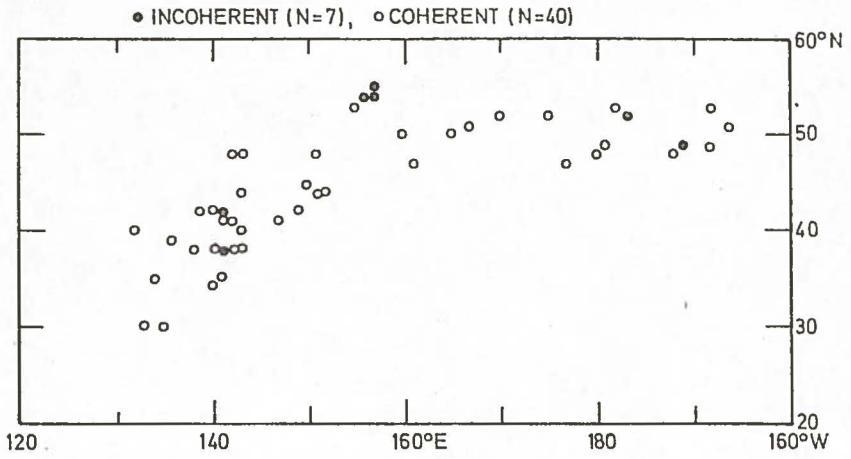

Fig 5. Events reported in the final NORSAR bulletin which were detected by either the coherent or the incoherent detector, but not by both. The time period covered is 16 Sept-15 Nov 1972, and typical SNR detection thresholds were 3.6 (coherent) and 1.6 (incoherent). The figure shows detection performance in the Aleutian-Kurile-Kamchatka-Japan area.

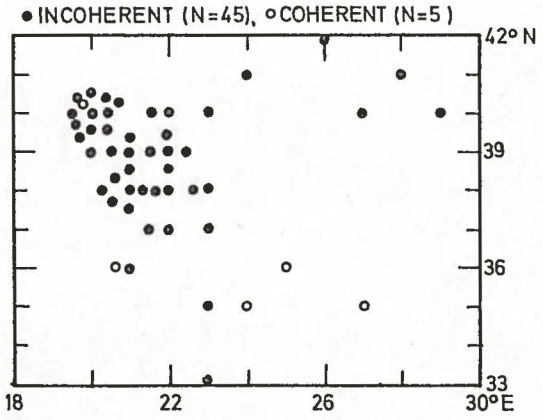

Fig 6. Same as Fig 5, but covers the Mediterranean area.

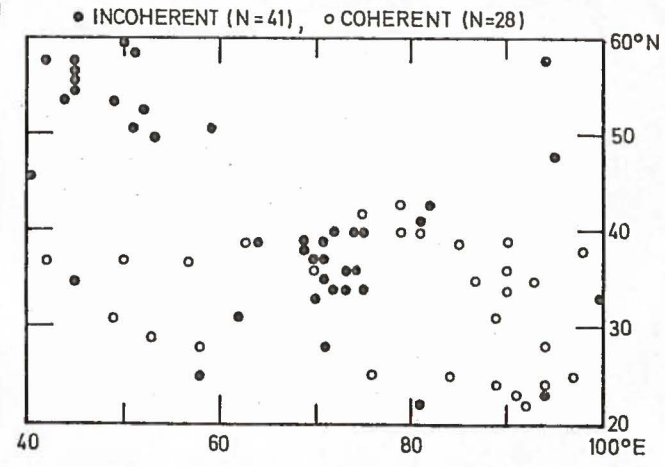

Fig 7. Same as Fig 5, but covers Russia and Central Asia.

To verify whether the signal amplitude distribution among NORSAR sensors is consistent with the theory developed in Section 5, nine different events were analyzed (see Table 2). For each event, the largest positive and negative amplitude values were extracted for each individual

EVENT NO.	DATE 1972	ORIGIN TIME (h min s)	LATITUDE deg	LONGITUDE deg	M_B	REGION
1	12 Aug	09 42 00	50.3N	177.8W	5.6	Aleutians
2	28 Aug	15 20 54	50.2N	178.1W	5.3	Aleutians
3	03 Jan	06 36 44	52.3N	158.4E	5.0	Kamchatka
4	24 Mar	22 56 18	51.7N	158.8E	5.0	Kamchatka
5	28 Mar	04 21 45	48.2N	80.4E	5.1	Kazakh
6	05 Apr	05 36 57	41.5N	142.3E	5.3	Japan
7	11 May	00 44 54	42.2N	143.9E	5.6	Japan
8	31 Mar	02 58 19	38.1N	21.8E	4.7	Greece
9	11 Apr	02 21 12	0.3N	29.3W	6.0	C. Mid-Atlantic Ridge

Table 2

Events used for analysis of sensor amplitude distribution. All epicenter parameters are as reported in the NORSAR seismic bulletin.

short period sensor. The amplitude data was then subjected to a statistical analysis performed by a Kolmogorov-Smirnov limiting distribution test. A specified theoretical distribution function being the hypothesis, the maximum difference D between the empirical and theoretical cumulative distribution function was computed. The statistic $Z = \sqrt{n} \cdot D$, where n is sample size, was used as a test value. Finally, the probability P_I of doing an error when rejecting the hypothesis was estimated. The theoretical distributions under consideration were: The normal (Gaussian), lognormal and exponential probability functions. Tables 3 and 4 give the scores obtained for the events listed in Table 2. Filters of 1.0-3.4 Hz and 1.4-3.8 Hz respectively were applied to the sensor traces prior to the amplitude measurements. The expectation and variance parameters required in the above hypothesis test, were estimated from the test sample and thus introduce a small

Event No.	Region	Period Sec.	No. Sensors	MB	Ampl.	NORMAL				LOG NORMAL				EXPONENTIAL			
						μ	σ	Z-Value	P_I%	μ	σ	Z-Value	P_I%	μ	σ	Z-Value	P_I%
1	Aleutians	1.0	120	5.6	Pos.	2028	1013	1.626	1.0	7.5027	0.5044	0.8417	47.8	2028	1013	1.187	12.0
					Neg.	2092	1104	0.9493	32.8	7.5009	0.5657	1.1150	16.6	2092	1104	1.643	0.9
2	Aleutians	0.8	132	5.3	Pos.	1143	567	1.132	15.4	6.9152	0.5210	0.8461	47.1	1143	567	1.828	0.3
					Neg.	1224	660	0.9130	37.5	6.9662	0.5552	0.9155	37.2	1224	660	1.752	0.4
3	Kamchatka	0.8	132	5.0	Pos.	618	356	1.269	8.0	6.2630	0.5851	0.8292	49.8	618	356	1.649	0.9
					Neg.	586	329	1.266	8.1	6.2170	0.5679	0.5979	86.7	586	329	1.900	0.1
4	Kamchatka	0.7	132	5.0	Pos.	850	489	1.493	2.3	6.5855	0.5660	0.8673	43.9	850	489	1.654	0.8
					Neg.	777	348	1.162	13.4	6.5305	0.5125	0.9407	33.9	777	384	2.002	0.1
5	Kazakh	0.6	132	5.1	Pos.	1644	892	1.333	5.7	7.2711	0.5187	0.6049	85.8	1644	892	1.393	4.1
					Neg.	1653	1062	2.078	0.0	7.2506	0.5468	0.8296	49.7	1653	1062	0.6418	80.5
6	Japan	0.9	132	5.3	Pos.	1566	928	1.393	4.1	7.1742	0.6228	0.9236	36.1	1566	928	1.741	0.5
					Neg.	1305	648	0.9942	27.6	7.0445	0.5269	1.087	18.8	1305	648	2.263	0.0
7	Japan	0.7	120	5.6	Pos.	2328	1226	0.9829	28.9	7.6103	0.5499	0.7352	65.2	2328	1226	2.100	0.0
					Neg.	2289	1143	1.114	16.7	7.6064	0.5275	0.8556	45.7	2289	1143	1.826	0.3
8	Greece	0.7	132	4.7	Pos.	712	410	2.089	0.0	6.4353	0.4988	0.9786	29.4	712	410	0.5576	91.5
					Neg.	797	486	2.141	0.0	6.5378	0.5104	1.4960	2.3	797	486	1.1820	12.2
9	C.Mid-Atlantic Ridge	1.6	126	6.0	Pos.	718	318	1.110	17.0	6.4753	0.4637	0.8882	40.9	718	318	1.693	0.6
					Neg.	690	327	1.089	18.6	6.4265	0.4787	0.5660	90.6	690	327	1.605	1.2

TABLE 3

Quality of fit scores for P-wave amplitude distributions obtained in Kolmogorov-Smirnov limiting distribution tests. μ=computed sample mean, σ=computed sample standard deviation, Z-value=test statistics, and P_I=probability assigned to the distribution by the above test. (Filter B-BP 1.0-3.4 Hz^I)

Event No.	Region	Period Sec.	No. Sensors	MB	Ampl	NORMAL				LOG NORMAL				EXPONENTIAL			
						μ	σ	Z-Value	P_I%	μ	σ	Z-Value	P_I%	μ	σ	Z-Value	P_I%
1	Aleutians	1.0	120	5.6	Pos.	1704	985	1.471	2.6	7.2884	0.5620	0.7117	69.2	1704	985	1.278	7.6
					Neg.	1645	909	1.328	5.9	7.2615	0.5510	0.9260	35.8	1645	909	1.461	2.8
2	Aleutians	0.8	132	5.3	Pos.	936	545	1.170	13.0	6.6833	0.5745	0.7070	70.0	936	545	1.594	1.2
					Neg.	970	535	1.008	26.2	6.7192	0.5863	0.7293	66.2	970	535	1.915	0.1
3	Kamchatka	0.8	132	5.0	Pos.	341	191	1.313	6.3	5.6744	0.5692	0.6565	78.2	341	191	2.678	0.1
					Neg.	347	195	1.280	7.6	5.6929	0.5718	0.8497	46.6	347	195	1.741	0.5
4	Kamchatka	0.7	132	5.0	Pos.	746	414	1.243	9.1	6.4613	0.5634	0.9061	38.4	746	414	2.097	0.0
					Neg.	742	409	1.621	1.0	6.4669	0.5379	0.7207	67.7	742	409	1.567	1.5
5	Kazakh	0.6	132	5.1	Pos.	1439	916	1.995	0.1	7.1070	0.5495	1.170	12.9	1439	916	1.150	14.2
					Neg.	1452	902	1.789	0.3	7.1298	0.5322	0.9525	32.4	1452	902	0.8457	47.2
6	Japan	0.9	132	5.3	Pos.	1244	733	1.651	0.9	6.9560	0.5942	0.8955	39.9	1244	733	1.567	1.5
					Neg.	1278	744	1.096	18.1	6.9871	0.5942	0.9153	37.2	1278	744	1.096	0.8
7	Japan	0.7	120	5.6	Pos.	2007	1198	1.121	16.2	7.4269	0.6153	0.5064	96.0	2007	1198	1.552	1.6
					Neg.	1828	950	1.107	17.2	7.3743	0.5377	0.6555	78.3	1828	950	1.917	0.1
8	Greece	0.7	132	4.7	Pos.	565	320	1.737	0.5	6.2094	0.4813	1.1142	14.7	565	320	0.7011	70.9
					Neg.	628	387	2.151	0.0	6.2944	0.5246	0.9666	30.8	628	387	0.6210	83.5
9	C. Mid-Atlantic Ridge	1.6	126	6.0	Pos.	367	187	1.372	4.6	5.7856	0.4931	0.4467	98.8	367	187	1.405	3.9
					Neg.	385	202	1.305	6.6	5.8212	0.5257	0.5098	95.7	385	202	1.425	3.4

TABLE 4

Quality of fit scores for P-wave amplitude distributions obtained in Kolmogorov-Smirnov limiting distribution tests. (Filter B-BP 1.4-3.8 Hz.) μ=computed sample mean, σ=computed sample standard deviation, Z-value=test statistics, and P_I=probability assigned to the distribution by the above test.

positive bias in the calculated significance levels (Lilliefors, 1967). However, this effect would be partly eliminated if we restrict ourselves to a comparative analysis of test values.

It should be noticed that the Kolmogorov-Smirnov test is not very stable for the small sample size used here. This is obvious from the great differences between the scores for positive and negative amplitude values, and has also been found when applying the test to samples of data whose distribution was known. Anyway, it is obvious from the tabulated results that the lognormal distribution provides a far better model for the observed amplitude variations than the other two, and in view of the above remarks, we conclude that the test results support our theoretical considerations presented in Section 5.

Considering the large and systematic spread in signal amplitudes across the array, a natural question is whether restricting the beamforming processing to a few good sensors could improve or match the performance of the full array. The detectability concepts defined in Section 4 have provided a convenient tool for investigating this problem. Several events were selected for this purpose, and the NORSAR sensors were ranked according to their amplitudes. Fig 8 shows an example of gain in event detectability when using the N best stations as a function of N.

It appears that the full array detectability is essentially achieved with less than one third of the sensors, assuming that the best ones have been selected. This holds true for both methods of beamforming. It seems, however, not to be possible to improve the array performance substantially by selective elimination of "low amplitude" sensors or subarrays. Also the fact that sensor performance is strongly dependent upon event location makes it difficult to draw advantages from the amplitude variations as to cost/performance tradeoff.

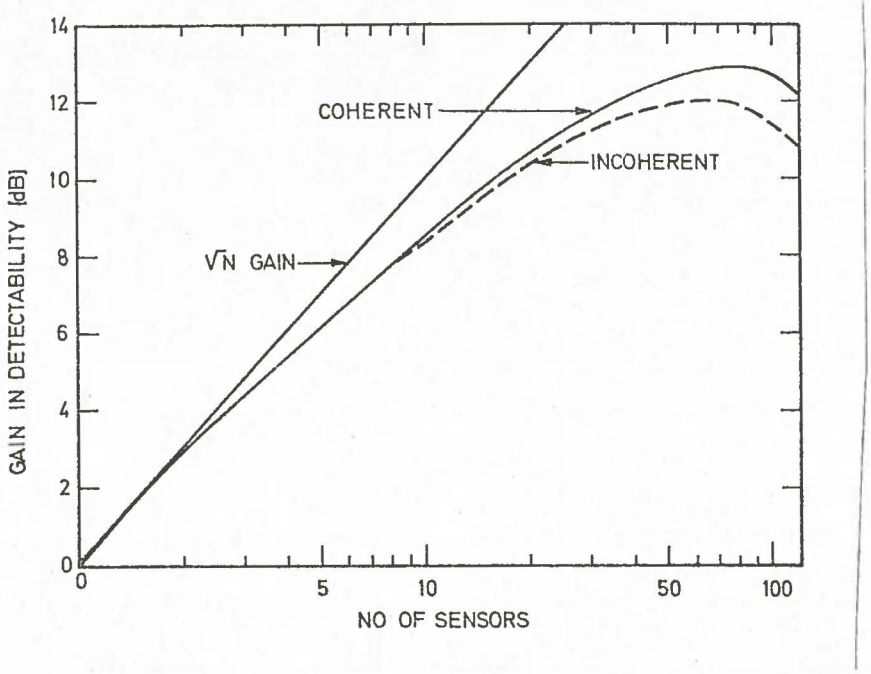

Fig 8. Gain in detectability (dB) as function of N when the N best sensors are selected for beamforming (coherent and incoherent). Observed NORSAR amplitudes (120 sensors) for Event No. 7 in Table 2 were used. Actual beamforming was not performed, instead eq. (9) (with q=0.8) and eq. (11) were used for detectability computations.

7. DISCUSSION

We have shown that incoherent beamforming is generally superior to conventional beamforming in detecting near regional seismic events, events which produce signals with low coherency across the array and very high frequency signals. The main disadvantages of the incoherent detector are its sensibility to local explosions, the poor location estimates caused by the broad main lobe of the beam and the fact that conventional beamforming is superior when it comes to detecting small, coherent seismic signals.

From a computer processing point of view, the incoherent detector has the advantage of providing adequate world coverage with very few array beams (less than 100 for

NORSAR), and the computational requirements are also small due to the low sampling rate for the signal envelopes. The lack of location precision is not a major handicap when off-line event analysis is available, as is the case at the NORSAR data center. In the NORSAR implementation, the incoherent detector has required only 20% of the computer main storage and computational load necessary for the conventional method. Thus as an alternative detector, the incoherent processor can achieve a substantial decrease in computer requirements while retaining most of the detection capability of the array. We still think that the major benefit of an incoherent detector is as a supplement to conventional beamforming especially designed to record events of high dominant frequency and underground explosions. Since explosions may occur at unpredictable sites, where no region corrections may be available for array beamforming, the broad main lobes of the incoherent beams make this method especially useful for detecting this type of seismic events, thereby providing a valuable tool for nuclear test monitoring. We would finally like to mention the interesting aspects of providing a world-wide multi-array seismic detection network using incoherent beamforming. For an outline of this idea, we refer to Husebye et al (1972).

REFERENCES

Berteussen, K-A.: Seismic event detection problems with special reference to the NORSAR array, Thesis, Bergen University, Bergen, Norway, 1972.

Bungum, H., E.S. Husebye and F. Ringdal: The NORSAR array and preliminary results of data analysis, Geophys. J. R. Astr. Soc., Vol. 25, pp. 115-126, 1971.

Edwards, J.P., S.A. Benno and G. Creasey: Evaluation of the CPO auxiliary processor, CPO Spec. Rep. No. 5, Texas Instruments Sci, Ser. Div., Dallas, Texas, U.S.A., 1967.

Felix, C.P., W.L. Gilbert and S.G. Wheeler: Preliminary results from the NORSAR system, Proceed. Seminar on Seismology and Seismic Arrays, NTNF/NORSAR, Kjeller, Norway, pp. 143-164, 1972.

Husebye, E.S., F. Ringdal and J. Fyen: On real-time processing of data from a global seismological network, NORSAR Tech. Rep. No. 43, NTNF/NORSAR, Kjeller, Norway, 1972.

Lacoss, R.T.: Variations of the false alarm rates at NORSAR, MIT, Lincoln Lab, 30 June 1972.

Lilliefors, H.W.: On the Kolmogorov-Smirnov test for normality with mean and variances unknown, J.A.S.A., Vol. 62, pp. 399-402, 1967.

Melton, B.S., and L.F. Bailey: Multiple Signal Correlators, Geophysics, Vol. 22, pp. 565-588, 1957.